Nanotechnology

DOI: 10.1002/anie.201201608

Macroscale Ordered Ultrathin Telluride Nanowire Films, and Tellurium/Telluride Hetero-Nanowire Films**

*Jian-Wei Liu, Jie Xu, Hai-Wei Liang, Kai Wang, and Shu-Hong Yu**

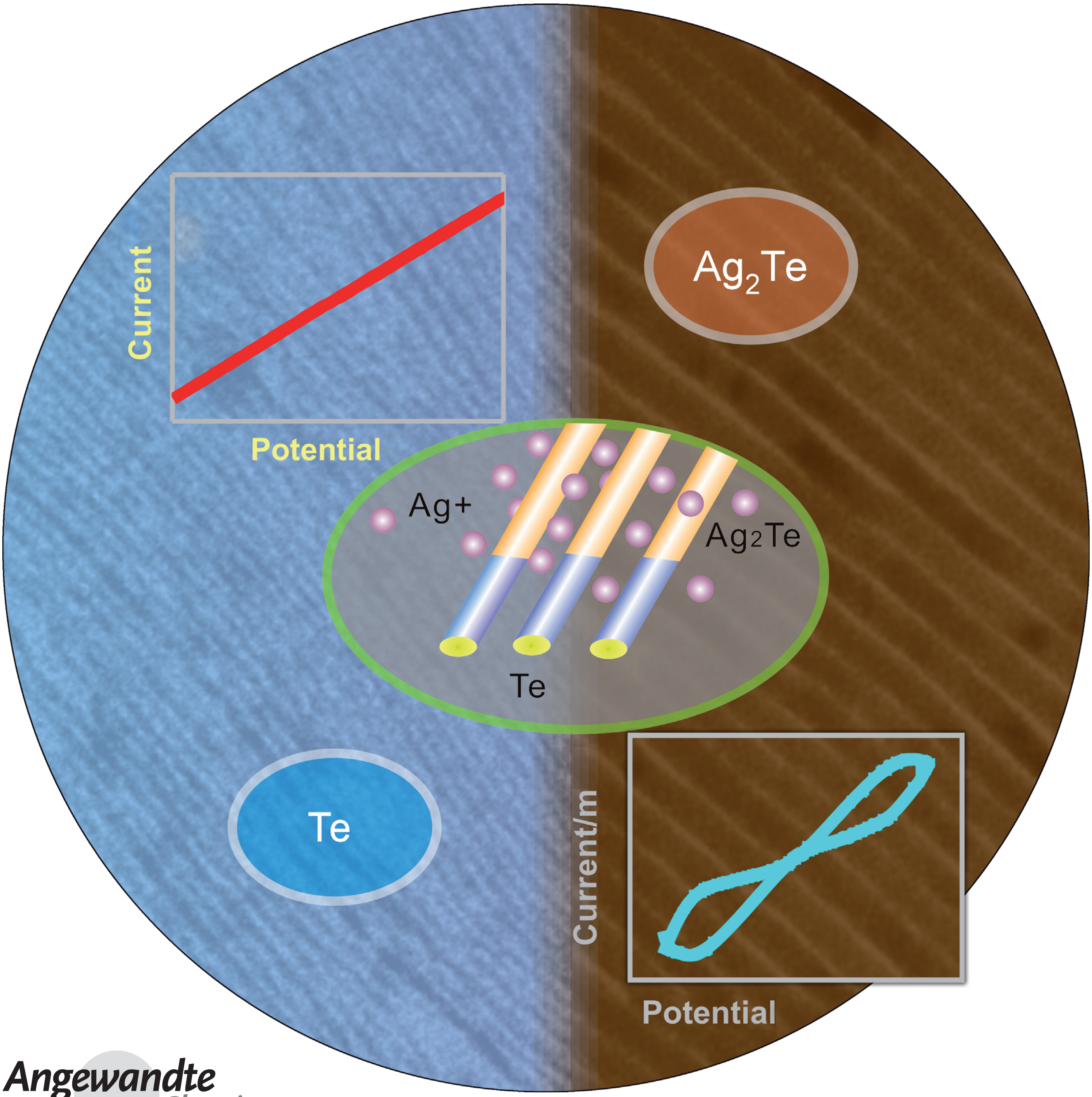

Within the past few decades, considerable attention has been paid to one-dimensional semiconductor nanowires because of their fundamental significance in basic scientific research and their potential applications; this has led to exciting developments in the field.[1–5] Recently, research has been gradually shifted from synthetic techniques to constructing well-defined, ordered superstructures. Assembling nanowires from a disordered to an ordered state within a desired system will provide insights into how the unique electrical, optical, magnetic, and spectroscopic properties of the nanowire assemblies can be exploited for potential applications.[6–8] The ability to control the self-assembly of ultrathin nanowires with ultrahigh aspect ratios will play an important role in the design of next-generation optoelectronic devices and other nanotechnologies. Various methods have been designed for the assembly of nanowires, including electric and dielectrophoresis,[9] magnetic-field-assisted alignment,[10] interface induced assembly,[11] microflow,[12] Langmuir Blodgett (LB) technique,[13,14] and others.[15–18] However, major efforts are still needed to further develop nanowire assembly approaches, especially for long and thin nanowires.

Elemental tellurium and telluride are well-known semiconductors with a narrow band-gap energy at room temperature that exhibit intriguing properties, such as unique photoconductivity, nonlinear optical response, high thermoelectric and piezoelectric responses; They have potential applications in gas sensors, optoelectronic devices, photonic crystal field-effect devices, self-developing holographic recording devices, radiative cooling devices, field-effect devices, and topological insulators.[19–23]

Herein, we demonstrate that macroscale ordered ultrathin telluride nanowire (NW) films (Ag_2Te, Cu_2Te, PbTe) and tellurium/telluride hetero-nanowire films (Te-Ag_2Te, Cu_2Te-Te-Ag_2Te-PbTe) can be rapidly fabricated using well-defined ultrathin single-crystalline TeNW patterns as templates through chemical transformation reactions. A well-aligned Ag_2TeNW film device shows bipolar, reversible, and non-volatile switching. During the process of pattern transferral, the electric property is shifted from the ohm character of the TeNW patterns to the memory effect of the Ag_2TeNW patterns. The chemical composition of the tellurium/telluride hetero-nanowire films can be easily controlled. This compositional change was revealed by electrical measurements during a series of sequential chemical transformations of a pattern formed on the same film. The photoconductive properties of the tellurium and telluride nanowire films suggest that they are sensitive to light, especially the ordered Cu_2Te nanowire films, for which the rise and decay times were less than 1 s. The clearly different behavior in the reactive patterns indicates that this strategy provides a new way for tailoring the properties of nanowires.

The assembly of nanowires is a crucial step toward their integration within devices. Monodisperse zero-dimensional spherical nanoparticles have been shown to easily self-organize into three-dimensional close-packed super-lattices. However, with an increase in aspect ratio, nanowires, especially ultrathin nanowires, become more difficult to self-assemble into structures with orientational and/or positional order. This is due to the extra possible configurations associated with these long and flexible nanostructures, such as curling and twisting.[24,25] Well-aligned Ag_2TeNWs with a diameter of about 9 nm and a length of several hundred of micrometers can be rapidly obtained by a pattern-transfer reaction using a template of well-aligned TeNWs with a diameter of about 7 nm and a length of several micrometers (Figure 1). First, TeNW arrays were obtained over a large area by the LB technique.[13] The color of the glass slides changed from dark blue to brown once the Te patterns were immersed in a $AgNO_3$ solution, and immediately converted into Ag_2TeNWs (Figure 1 a,e; see also the video in the Supporting Information). The composition of the Ag_2TeNW film was confirmed by energy dispersive X-ray spectroscopy (EDS) and X-ray photoelectron spectroscopy (XPS) (Supporting Information, Figure S1). The degree of order in the Ag_2TeNW assembly is determined by the TeNW assembly. Figure 1 b,f show TEM images of Te and Ag_2TeNW patterns of the corresponding glass slides (Figure 1 a,e) made for small angle X-ray diffraction pattern (SAXRD) measurements (Figure 1 c,g). TEM images give intuitive periodic information on the structures, while the electron diffraction gives indirect periodic information. Referring to the SAXRD and TEM images, the period of the TeNW monolayer (about 6.8 nm) was transferred to Ag_2TeNW monolayer (about 8.9 nm). Such a period varies with the diameters of the TeNWs. Figure 1 d,h show the UV–Vis spectra of the Te nanowire monolayer and Ag_2TeNW monolayer, respectively. These display typical absorption peaks located at 586 nm and 450 nm, respectively, indicating an optical change from the pattern transfer process. When the UV–Vis spectrum of the ordered TeNW monolayer on a quartz substrate is compared with the TeNWs in aqueous solution, a red-shift in the surface plasmon resonance indicates an increase in order. The crystal quality of Te and

---

[*] J.-W. Liu, J. Xu, H.-W. Liang, K. Wang, Prof. Dr. S. H. Yu
Division of Nanomaterials and Chemistry, Hefei National Laboratory for Physical Sciences at the Microscale, Department of Chemistry, National Synchrotron Radiation Laboratory, University of Science and Technology of China
Hefei, Anhui: 230026 (P.R. China)
E-mail: shyu@ustc.edu.cn
Homepage: http://staff.ustc.edu.cn/~yulab/

[**] We acknowledge funding support from the National Basic Research Program of China (2010CB934700), the National Natural Science Foundation of China (91022032, 21061160492, J1030412), the Chinese Academy of Sciences (KJZD-EW-M01-1), the International Science & Technology Cooperation Program of China (2010DFA41170), and a Principal Investigator Award from the National Synchrotron Radiation Laboratory at the University of Science and Technology of China. J.W.L. thanks the USTC Special Grant for Postgraduate Research, Innovation and Practice, and the CAS Special Grant for Postgraduate Research, Innovation and Practice, as well as the Fundamental Research Funds for the Central Universities (2340000033). We thank Dr. Y. P. Yao and Prof. X. G. Li at the Hefei National Laboratory for Physical Sciences at the Microscale for their helpful discussions and help in the measurement of the memory properties of the nanowire thin films.

Supporting information for this article, including the experimental section, a video for the transformation reaction from tellurium nanowires to silver telluride nanowires, and TEM images of the *I–V* characteristics, is available on the WWW under http://dx.doi.org/10.1002/anie.201201608.

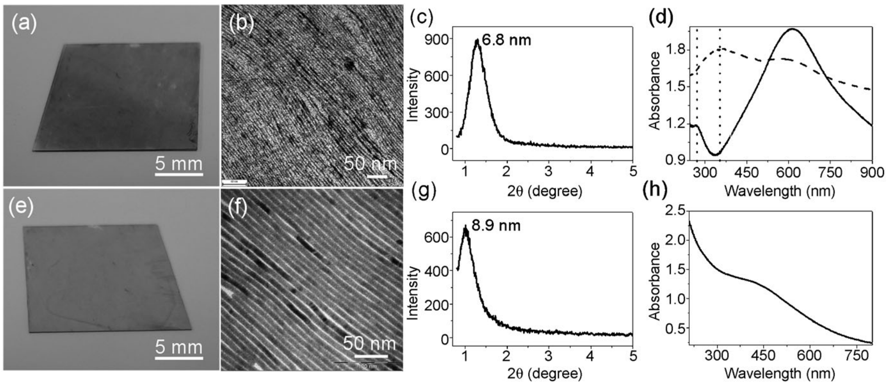

Figure 1. (a,e) Photographs of ordered Te and Ag_2TeNW monolayers, respectively, on glass slides. (b,f) TEM images of Te and Ag_2TeNW monolayers, respectively. (c,g) SAXRD spectrums of ordered Te and Ag_2TeNW monolayers, respectively, on the glass slide. (d) UV–Vis spectrum of Te nanowires in aqueous solution (——), and an ordered Te nanowire monolayer on a quartz substrate (-----). (h) UV–Vis spectrum of a Ag_2TeNW monolayer generated from a TeNW monolayer.

Ag_2Te nanowires before and after ion-exchange reactions were confirmed by TEM and HRTEM (Supporting Information, Figure S2).

The most essential feature of resistance memory is the field-direction dependence, meaning that the resistance of the system can be switched by applied voltage or current pulses associated with current–voltage (I–V) hysteresis. A 15-layer parallel assembly of Ag_2TeNW films can be fabricated onto a Si/SiO_2 (SiO_2 layer thickness = 500 nm) substrate by the pattern transfer method, and a promising memory device based on resistive switching behavior can be constructed (Supporting Information, Figure S3). The working electrode was made by depositing 5 nm of Ti onto a SiO_2 wafer followed by a 100 nm layer of Au. The electrical properties of the nano-devices were investigated with a PM5 Analytical Probe System (Cascade Microtech, Inc.) and a Keithley 4200 SCS in a clean, metal-shielded box at room temperature in air. The ordered TeNW films exhibit a linear behavior, and thus feature an ohmic contact (see Figure 3 d).[13] Figure 2 a shows ten consecutive cycles of I–V measurements on the nanowire device conducted at room temperature, as well as the direction of the applied pulse voltage. The bias voltage was swept from $-V_{max}$ to $+V_{max}$ followed by a reverse from $+V_{max}$ to $-V_{max}$. Figure 2 b shows the I–V curves with the current in a logarithmic scale. All of the curves are symmetric and nonlinear, indicating that the current at the probe voltage for the high-conducting state is higher than that of the current in the low-conducting state at the same voltage. The endurance of the resistive switching can be enhanced by further increasing the sweeping voltage (Supporting Information, Figure S4). The electric pulses (pulse width = 100 ms, ± 8 V) were applied and Figure 2 c shows that the devices give fairly reproducible results for the positive and negative switching phenomena. Here a + 8 V and −8 V pulse (0.1 s) induced the respective states, while 5 mV pulse acted as the read pulse. To estimate the stability of the switch states, we probed them by continuously applying electric pulses for 2000 cycles. The results show that the nanowire memory device showing no state disturbance (no overlap between the high resistance state (HRS) and the low resistance state (LRS)), even after about 2000 cycles. The device, which consists of well aligned Ag_2TeNW films, displays a bipolar, reversible, and nonvolatile switching of structures, with a ratio of 3.8:1 for ON/OFF conductance. In 1971, the concept of the memory-resistor (memristor) was postulated by Chua through the analysis of the mathematical relations between pairs of fundamental circuit variables.[26] Ultimately, the dynamic properties of the electrons and ions are the physical origin of memory.[27] Memory effects are ubiquitous in nature and are particularly relevant at the nanoscale, where many comprehensive and impressive reviews have been given on this topic.[27–30] The reversible I–V of the Au/Ag_2Te/Au systems can be explained by vacancy migration under an applied electric field, judging from the resistance changes from LRS to HRS in the positive bias. A negative voltage accumulates vacancies at the interface, which results in the lowering of the Schottky-like barrier height and width.[31]

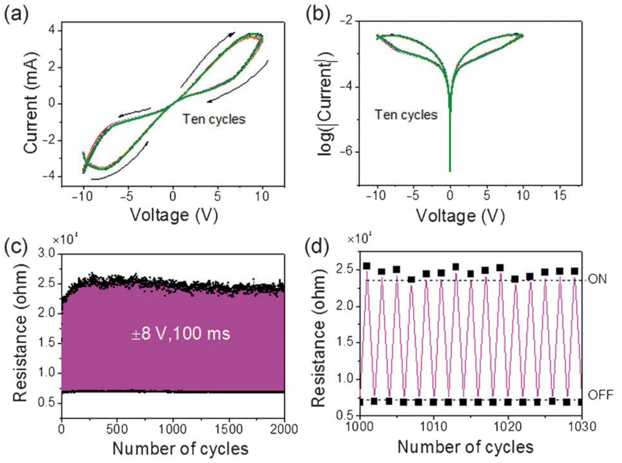

Figure 2. (a) Current–voltage characteristics of 15 layers of well-patterned Ag_2TeNW films in two voltage sweep directions, from −10 to +10 V and from +10 to −10 V. (b) the I–V curves with the current in a logarithmic scale. (c) Read-only memory applications over about 2000 cycles. The magnitude of the current under a probe voltage pulse is plotted as a function of time after high and low states were induced by applying pulses of −8 and +8 V (width 0.1 s), respectively. (d) Read-only memory applications from 1000 to 1030.

Cation exchange reactions are widely used to alter the composition and properties of the material by replacing the cations within the nanocrystal lattice with a different metal ion.[32–34] Figure 3 a shows an illustration of the compositional control of a nanowire monolayer oriented by chemical transformation. The pattern transfer process can be promoted directly on a variety of substrates, such as glass, quartz, silicon, polymers, even filter paper (Figure 3 b). As shown in Fig-

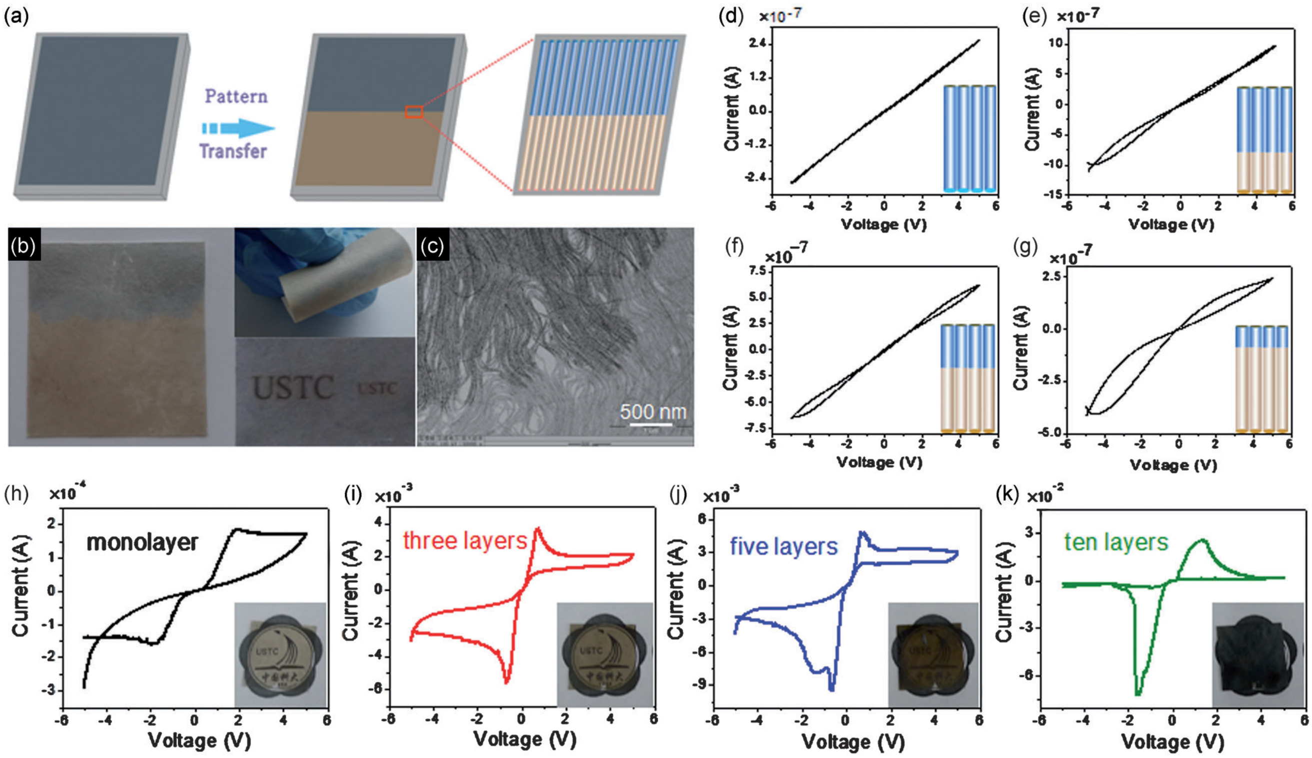

Figure 3. (a) Illustration of compositional control by the chemical transformation of an oriented nanowire monolayer. (b) Photograph of a pattern transfer monolayer on a flexible substrate. (c) TEM image of a Te-Ag_2Te hetero-nanowire monolayer. (d–g) A series of sequential measurements on the same nanowire films; the surface areas of Ag_2Te relative to Te are (d) 0%, (e) 40%, (f) 60%, and (g) 80%. (h–k) Current-voltage characteristics from −5 to +5 V and from +5 to −5 V of well-patterned Ag_2TeNW films composed of (h) monolayer, (i) three layers, (j) five layers, and (k) ten layers. The insets are photographs of the corresponding Ag_2Te films on glass slides.

ure 3b, the films are flexible, glossy, and very smooth. Moreover, brown Ag_2TeNW patterns were easily drawn on the dark blue TeNW film using an aqueous $AgNO_3$ solution as ink, indicating that the pattern transfer process is a versatile method. To demonstrate the high degree of compositional control, we took electrical measurements of the same nanowire films during a series of sequential chemical transformation pattern transfers (Figure 3d–g). Figure 3d–g shows that the I–V curves of the sample showed a memory phenomenon as the surface area of Ag_2Te relative to Te goes from 0% to 80%, for both Te-Ag_2Te hetero-nanowire films and pure Ag_2Te. The demarcation line of the Te-Ag_2Te hetero-nanowire film shifts slightly under the TEM electron beam (Supporting Information, Figure S5), and can be explained by silver ion movement under electron-beam irradiation.[35] To investigate the memory characteristics of the Ag_2TeNW films in detail, a series of devices composed of one, three, five, or ten Ag_2Te monolayers were fabricated (Figure 3h–k). As the number of Ag_2Te nanowire layers increases, the current of the device increases and the memory loops become more obvious.

To make the pattern transfer strategy more versatile and to assess the potential applicability of tellurium and tellurides as photoconductive materials, we generated a Cu_2TeNW film from an ordered TeNW monolayer and a PbTeNW film from a Ag_2TeNW monolayer, as examples. Figure 4a shows photographs of telluride hetero-nanowire films, which start from TeNWs. These are converted into Te-Ag_2Te hetero-nanowire films, then Cu_2Te-Te-Ag_2Te hetero-nanowire films, and finally Cu_2Te-Te-Ag_2Te-PbTe hetero-nanowire films. The reactions were indicated by a color change on the nanowire film. Elemental tellurium is a well-known p-type helical semiconductor with a narrow band-gap energy of 0.35 eV at room temperature, and the photoconduction of Te nanowires has been studied previously.[13,19] The photoelectric properties of the tellurium and telluride hetero-nanowire nano-device were investigated with a Cascade Microtech PM5 analytical probe system and a Keithley 4200 SCS in a clean, metal-shielded box at room temperature in air. The electrical resistance of the nanowire films changed when illuminated, which is similar to other photoconductive materials. Figure 4b–e shows the reversible switching of the nanowire devices between low and high conductivity states, as the lamp was turned off and on, for monolayer films from TeNWs, Cu_2TeNWs, Ag_2TeNWs, and PbTeNWs, respectively. The bias on the nanowires was 0.1 mV, and the light intensity was 5.76 mW cm^{-2}. The photoconductive properties of the telluride nanowire films suggest that they are sensitive to light, especially for the ordered Cu_2TeNW monolayer, whose rise and decay times were less than 1 s (Supporting Information, Figure S6). After the test cycles, the switch ratio remained stable, indicating that they are candidates for optoelectronic switches.

Based on previous work,[36–39] these Ag_2TeNW patterns can be converted into CdTe and ZnTeNW patterns using

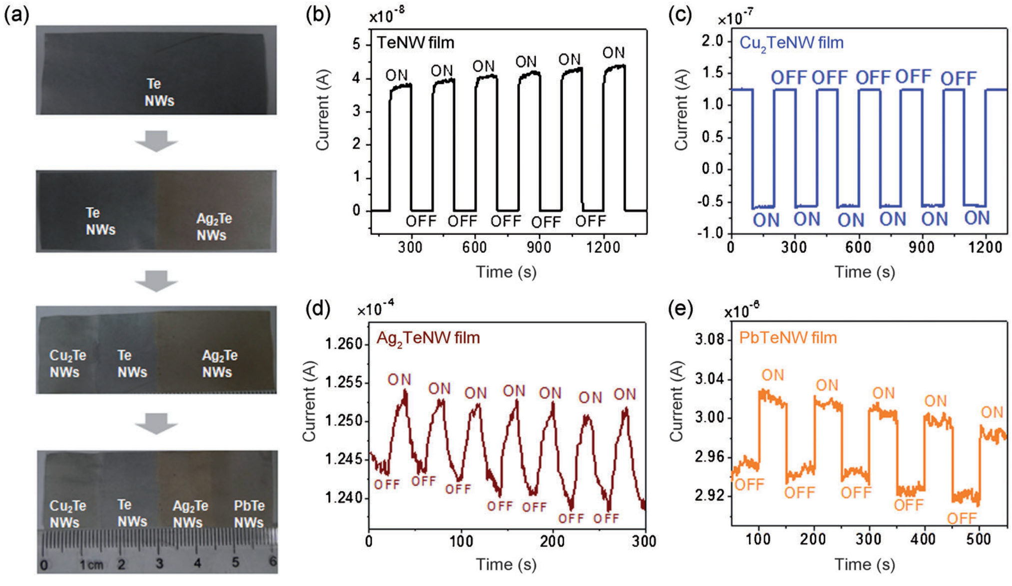

Figure 4. (a) Photographs of the sequential chemical conversion of a TeNW monolayer into Te-Ag_2TeNW films, Cu_2Te-Te-Ag_2TeNW films, and Cu_2Te-Te-Ag_2Te-PbTeNW films. (b–e) Reversible switching of different telluride nanowire patterns between low and high conductivity states as the light is turned on and off. The bias on the nanowire films is 0.1 mV.

cation-exchange reactions, and the CdTeNW patterns can be further transformed into $PtTe_2$ nanotubes, which could find other applications in the field.

In conclusion, we have demonstrated that the original chemically reactive nanowire patterns can act first as reducing agents, and then as templates for directing the connectivity and arrangement of newly transformed inorganic 1D nanowires. Macroscale ultrathin telluride nanowire films, such as Ag_2Te, Cu_2Te, and PbTe, can be rapidly fabricated by chemical transformation at room temperature. Furthermore, this versatile strategy can also be used to fabricate tellurium/telluride hetero-nanowire films (Te-Ag_2Te and Cu_2Te-Te-Ag_2Te-PbTe). The properties of the ultrathin hetero-nanowire films obtained could also be tuned by changing the composition of the hetero-nanowire films through chemical transformation. Well-defined parallel Ag_2TeNW films with high ordering can be fabricated into a stable memory device with a resistive switching behavior. More importantly, the presented pattern transfer process by chemical transformation provides a new means to access a family of other macroscale ultrathin nanowire thin films, or their hetero-nanowire thin film counterparts, by taking advantage of high reactivity of ultrathin TeNWs. This method is expected to find broad application in nanodevices in the future.

Received: February 28, 2012
Revised: April 30, 2012

Keywords: nanostructures · nanowires · semiconductors · telluride · tellurium

[1] D. Appell, *Nature* **2002**, *419*, 553–555.
[2] S. Xu, Y. Qin, C. Xu, Y. G. Wei, R. S. Yang, Z. L. Wang, *Nat. Nanotechnol.* **2010**, *5*, 366–373.
[3] A. I. Hochbaum, P. D. Yang, *Chem. Rev.* **2010**, *110*, 527–546.
[4] P. D. Yang, R. X. Yan, M. Fardy, *Nano Lett.* **2010**, *10*, 1529–1536.
[5] P. Caroff, K. A. Dick, J. Johansson, M. E. Messing, K. Deppert, L. Samuelson, *Nat. Nanotechnol.* **2009**, *4*, 50–55.
[6] M. Yaman, T. Khudiyev, E. Ozgur, M. Kanik, O. Aktas, E. O. Ozgur, H. Deniz, E. Korkut, M. Bayindir, *Nat. Mater.* **2011**, *10*, 494–501.
[7] H. Yan, H. S. Choe, S. W. Nam, Y. J. Hu, S. Das, J. F. Klemic, J. C. Ellenbogen, C. M. Lieber, *Nature* **2011**, *470*, 240–244.
[8] J. W. Liu, H. W. Liang, S. H. Yu, *Chem. Rev.* **2012**, DOI: 10.1021/cr-2011-00347w.
[9] E. M. Freer, O. Grachev, X. F. Duan, S. Martin, D. P. Stumbo, *Nat. Nanotechnol.* **2010**, *5*, 625–625.
[10] B. Wang, Y. F. Ma, N. Li, Y. P. Wu, F. F. Li, Y. S. Chen, *Adv. Mater.* **2010**, *22*, 3067–3070.
[11] H. Y. Shi, B. Hu, X. C. Yu, R. L. Zhao, X. F. Ren, S. L. Liu, J. W. Liu, M. Feng, A. W. Xu, S. H. Yu, *Adv. Funct. Mater.* **2010**, *20*, 958–964.
[12] Y. Huang, X. F. Duan, Q. Q. Wei, C. M. Lieber, *Science* **2001**, *291*, 630–633.
[13] J. W. Liu, J. H. Zhu, C. L. Zhang, H. W. Liang, S. H. Yu, *J. Am. Chem. Soc.* **2010**, *132*, 8945–8952.
[14] A. Tao, F. Kim, C. Hess, J. Goldberger, R. R. He, Y. G. Sun, Y. N. Xia, P. D. Yang, *Nano Lett.* **2003**, *3*, 1229–1233.
[15] F. Xu, J. W. Durham, B. J. Wiley, Y. Zhu, *ACS Nano* **2011**, *5*, 1556–1563.
[16] A. Pevzner, Y. Engel, R. Elnathan, T. Ducobni, M. Ben-Ishai, K. Reddy, N. Shpaisman, A. Tsukernik, M. Oksman, F. Patolsky, *Nano Lett.* **2010**, *10*, 1202–1208.
[17] Z. Y. Fan, J. C. Ho, Z. A. Jacobson, R. Yerushalmi, R. L. Alley, H. Razavi, A. Javey, *Nano Lett.* **2008**, *8*, 20–25.
[18] A. Pevzner, Y. Engel, R. Elnathan, A. Tsukernik, Z. Barkay, F. Patolsky, *Nano Lett.* **2012**, *12*, 7–12.
[19] Y. Wang, Z. Y. Tang, P. Podsiadlo, Y. Elkasabi, J. Lahann, N. A. Kotov, *Adv. Mater.* **2006**, *18*, 518–522.
[20] D. Kong, Y. Cui, *Nat. Chem.* **2011**, *3*, 845–849.
[21] D. Kong, Y. Chen, J. J. Cha, Q. Zhang, J. G. Analytis, K. Lai, Z. Liu, S. S. Hong, K. J. Koski, S.-K. Mo, Z. Hussain, I. R. Fisher, Z.-X. Shen, Y. Cui, *Nat. Nanotechnol.* **2011**, *6*, 705–709.
[22] K. Wang, H. W. Liang, W. T. Yao, S. H. Yu, *J. Mater. Chem.* **2011**, *21*, 15057–15062.
[23] P. Tangney, S. Fahy, *Phys. Rev. B* **2002**, *65*, 054302.
[24] D. A. Triplett, L. M. Quimby, B. D. Smith, D. Hernández Rodríguez, S. K. St. Angelo, P. González, C. D. Keating, K. A. Fichthorn, *J. Phys. Chem. C* **2010**, *114*, 7346–7355.
[25] K. Sakakibara, J. P. Hill, K. Ariga, *Small* **2011**, *7*, 1288–1308.

[26] L. O. Chua, *IEEE Trans. Circuit Theory* **1971**, *18*, 507–519.
[27] M. Di Ventra, Y. V. Pershin, *Mater. Today* **2011**, *14*, 584–591.
[28] J. C. Scott, L. D. Bozano, *Adv. Mater.* **2007**, *19*, 1452–1463.
[29] Y. V. Pershin, M. Di Ventra, *Adv. Phys.* **2011**, *60*, 145–227.
[30] A. Sawa, *Mater. Today* **2008**, *11*, 28–36.
[31] K. Shibuya, R. Dittmann, S. B. Mi, R. Waser, *Adv. Mater.* **2010**, *22*, 411–414.
[32] D. H. Son, S. M. Hughes, Y. D. Yin, A. P. Alivisatos, *Science* **2004**, *306*, 1009–1012.
[33] B. Sadtler, D. O. Demchenko, H. Zheng, S. M. Hughes, M. G. Merkle, U. Dahmen, L. W. Wang, A. P. Alivisatos, *J. Am. Chem. Soc.* **2009**, *131*, 5285–5293.
[34] J. M. Luther, H. M. Zheng, B. Sadtler, A. P. Alivisatos, *J. Am. Chem. Soc.* **2009**, *131*, 16851–16857.
[35] M. Pang, J. Hu, H. C. Zeng, *J. Am. Chem. Soc.* **2010**, *132*, 10771–10785.
[36] H. W. Liang, S. Liu, S. H. Yu, *Adv. Mater.* **2010**, *22*, 3925–3937.
[37] H. W. Liang, S. Liu, Q. S. Wu, S. H. Yu, *Inorg. Chem.* **2009**, *48*, 4927–4933.
[38] H. W. Liang, S. Liu, J. Y. Gong, S. B. Wang, L. Wang, S. H. Yu, *Adv. Mater.* **2009**, *21*, 1850–1854.
[39] G. D. Moon, S. Ko, Y. Xia, U. Jeong, *ACS Nano* **2010**, *4*, 2307–2319.